

AD-A265 865



2

PL-TR-91-2197

Environmental Research Papers, No. 1092

**EFFECTS OF ABSORPTION ON HIGH
LATITUDE METEOR SCATTER COMMUNICATION SYSTEMS**

J.C. Ostergaard
J.A. Weitzen
P.A. Kossey
A.D. Bailey
P.M. Bench

S.W. Li
J.R. Katan
A.J. Coriaty
J.E. Rasmussen

DTIC
ELECTE
JUN 08 1993
S A D

31 July 1991

APPROVED FOR PUBLIC RELEASE; DISTRIBUTION UNLIMITED




**PHILLIPS LABORATORY
AIR FORCE SYSTEMS COMMAND
HANSCOM AIR FORCE BASE, MA 01731-5000**

93-12724

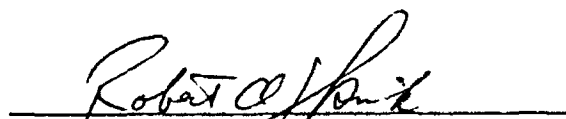


93 12724

"This technical report has been reviewed and is approved for publication"


JOHN E. RASMUSSEN
Branch Chief

FOR THE COMMANDER


ROBERT A. SKRIVANEK
Division Director

This report has been reviewed by the ESD Public Affairs Office (PA) and is releasable to the National Technical Information Service (NTIS).

Qualified requestors may obtain additional copies from the Defense Technical Information Center. All others should apply to the National Technical Information Service.

If your address has changed, or if you wish to be removed from the mailing list, or if the addressee is no longer employed by your organization, please notify GL/IMA, Hanscom AFB, MA 01731. This will assist us in maintaining a current mailing list.

Do not return copies of this report unless contractual obligations or notices on a specific document requires that it be returned.

REPORT DOCUMENTATION PAGE

Form Approved
OMB No 0704-0188

Public reporting burden for this collection of information is estimated to average 1 hour per response, including the time for reviewing instructions, searching existing data sources, gathering and maintaining the data needed, and completing and reviewing the collection of information. Send comments regarding this burden estimate or any other aspect of this collection of information, including suggestions for reducing this burden, to Washington Headquarters Services, Directorate for Information Operations and Reports, 1215 Jefferson Davis Highway, Suite 1204, Arlington, VA 22202-4302, and to the Office of Management and Budget, Paperwork Reduction Project (3704-0188), Washington, DC 20503.

1. AGENCY USE ONLY (Leave Blank)		2. REPORT DATE 1991 July 31		3. REPORT TYPE AND DATES COVERED Scientific, Interim	
4. TITLE AND SUBTITLE EFFECTS OF ABSORPTION ON HIGH LATITUDE METEOR SCATTER COMMUNICATION SYSTEMS				5. FUNDING NUMBERS PE - 62101F PR - 4643 TA - 10 WU - 08	
6. AUTHOR(S) J.C. Ostergaard*, J.A. Weitzen*, P.A. Kossey, A.D. Bailey, P.M. Bench, S.W. Li*, J.R. Katan*, A.J. Coriary, J.E. Rasmussen					
7. PERFORMING ORGANIZATION NAME(S) AND ADDRESS(ES) Phillips Laboratory (LID) Hanscom AFB, MA 01731-5000				8. PERFORMING ORGANIZATION REPORT NUMBER PL-TR-91-2197 ERP, No. 1092	
9. SPONSOR MONITORING AGENCY NAME(S) AND ADDRESS(ES)				10. SPONSORING MONITORING AGENCY REPORT NUMBER	
11. SUPPLEMENTARY NOTES *University of Lowell, Ctr. for Atmospheric Rsch., Lowell, MA. # Naval Underwater Systems Center, New London, CT					
12a. DISTRIBUTION AVAILABILITY STATEMENT Approved for public release; distribution unlimited				12b. DISTRIBUTION CODE	
13. ABSTRACT (maximum 200 words) Data acquired with the Geophysics Laboratory's High Latitude Meteor Scatter Test-Bed between Sondrestrom AB and Thule AB, Greenland during the solar disturbances of March and August, 1989 are presented. These disturbances provided a unique opportunity to observe a number of naturally occurring disturbance effects on meteor scatter links operated in the frequency range (35 to 147 MHz) covered by the test-bed. The disturbances range from signal absorption to system noise variations. The properties of ionospheric absorption in general are discussed and illustrated with computations using electron density profiles from the September 1978 Solar Proton Event. It has been found that accurate measurements of high levels of ionospheric absorption with riometers pose special problems. These problems are identified and discussed. The data acquired during the March and August solar disturbances are then related to the zenith absorption measured at Thule and the influence of absorption, as well as system noise variations are discussed. The two events presented are very different. The August event was dominated by ionospheric absorption and meteoric arrival rates and duty cycles were affected most on the lower frequencies 35 and 45 MHz although some effects could also be seen at the higher frequencies 65-147 MHz. The March event combined weak ionospheric absorption with large solar noise bursts. The effects of the event on the test-bed were dominated by increased solar noise at all frequencies. It is speculated as to whether solar noise bursts during previous SPE's have caused a different frequency dependence than the one expected due to signal absorption of the availability of the meteor scatter channel during disturbances.					
14. SUBJECT TERMS Meteor scatter High latitude Propagation Communication Absorption				15. NUMBER OF PAGES 34	
				16. PRICE CODE	
17. SECURITY CLASSIFICATION OF REPORT UNCLASSIFIED	18. SECURITY CLASSIFICATION OF THIS PAGE UNCLASSIFIED	19. SECURITY CLASSIFICATION OF ABSTRACT UNCLASSIFIED	20. LIMITATION OF ABSTRACT SAR		

NSN 7540-01-280-5500

Standard Form 298 (Rev. 2-89)
Prescribed by ANSI Std. Z39-18
298-102

DTIC QUALITY INSPECTED 8

Accession For	
NTIS CRA&I	<input checked="" type="checkbox"/>
DTIC TAB	<input type="checkbox"/>
Unannounced	<input type="checkbox"/>
Justification	
By	
Distribution /	
Availability Codes	
Dist	Avail and/or Special
A-1	

Contents

1. INTRODUCTION	1
2. IONOSPHERIC ABSORPTION AT VHF FREQUENCIES	4
3. MEASUREMENT OF IONOSPHERIC ABSORPTION AT VHF	11
4. THE INFLUENCE OF PCA'S ON SYSTEM NOISE	14
5. THE AUGUST 1989 PCA	15
6. THE MARCH 1989 PCA	22
7. SUMMARY	27

Figures

1 Geographical Locations of the GL High Latitude Meteor Scatter Test-Bed.	2
2 Cross Section of a Meteor Scatter Propagation Path.	3
3 Ratio of Path Length at Zenith and at Zenith Angles in the Range 0 to 90 Deg. Through the Ionosphere's D-region.	4
4 Electron Density Profiles at Noon on 23 and 26 Sept. 1978 at Thule.	6
5 Computed Cumulative Zenith Absorption at Noon 23 Sep. 1978.	7
6 Computed Specific Zenith Absorption at Noon 23 Sep. 1978.	7
7 Computed Cumulative Zenith Absorption at Noon 26 Sep. 1978.	8
8 Computed Specific Zenith Absorption at Noon 26 Sep. 1978.	8
9 Computed Frequency Dependence of the Cumulative Absorption at Noon 23 Sep. 1978.	9
10 Computed Frequency Dependence of the Cumulative Absorption at Noon 26 Sep. 1978.	9
11 Computed Exponent of Frequency Dependence of Absorption vs. Height at Noon 23 Sep. 1978.	10
12 Computed Exponent of Frequency Dependence of Absorption vs. Height at Noon 26 Sep. 1978.	10
13 Computed Radiation Pattern for the Riometer at Thule AB.	13
14 Ratio of Measured Absorption and Zenith Absorption in dB at Thule AB.	13
15 Computed Radiation Pattern for the 45 MHz Meteor Scatter Antenna at Thule AB.	15
16 Zenith Absorption Measured at Thule AB, 10 to 22 Aug. 1989.	16
17 Measured Noise Absorption at 35, 45, 65, 104, and 147 MHz at Thule AB, Aug. 1989.	17
18 Meteor Trail Arrival Rate Exceeding -116 dBm Signal Level at Thule AB, Aug. 1989.	19

19	Duty Cycle Exceeding -116 dBm at 35, 45, 65, 104, and 147 MHz at Thule Aug. 1989.	20
20	Duty Cycle and Frequency of Operation for Optimum Selection of Frequency Compared to Zenith Absorption 10 to 20 Aug. 1989.	21
21	Zenith Absorption Measured at Thule AB March 1989.	22
22	Measured Noise Absorption at 35, 45, 65, 85, 104, and 147 MHz Thule AB, March 1989.	23
23	Meteor Trail Arrival Rate Exceeding -116 dBm Signal Level at 35, 45, 65, 85, 104, and 147 MHz Thule AB, August 1989.	25
24	Duty Cycle Exceeding -116 dBm Signal Level at 35, 45, 65, 85, 104, and 147 MHz Thule AB, August 1989.	26

Effects of Absorption on High Latitude Meteor Scatter Communication Systems

1. INTRODUCTION

Polar Cap Absorption (PCA) events are caused by high energy (> 10 MeV) protons of solar origin, emanating from the sun during Solar Proton Events (SPE's). The particles are funnelled into the polar cap ionosphere along the earth's magnetic field lines creating increased ionization at altitudes between 45 and 90 km. The collision frequency in this part of the ionosphere is high, and the increased ionization causes absorption of radio waves passing through this region. The absorption is a function of frequency and the path length within the absorbing medium. Lower frequencies are absorbed more than higher frequencies and the absorption increases with path length.

The increased ionization caused by SPE's influences all radiowaves passing through the D-region of the ionosphere. Medium- and Shortwave communication systems can be severely influenced or even interrupted due to absorption. Meteor scatter systems operating in the VHF band are expected to suffer less due to the lower level of absorption at these frequencies. Information confirming the existence of PCA influence on meteor scatter links exists^{1,2}, but no extensive, quantitative evaluation of these effects over the frequency range of 30-150 MHz used for meteor scatter communication has been undertaken.

The Air Force's Geophysics Laboratory (GL) operates a 1200 km diagnostic meteor scatter link between Sondrestrom AB and Thule AB, Greenland. The link is situated entirely within the Polar Cap and operates at 35, 45, 65, 85, 104, and 147 MHz, as shown in Figure 1. A second diagnostic link between Sondrestrom AB and Narssarssuaq in southern Greenland is 700 km long. This link passes through the auroral oval and operates at 45, 65, 85, and 104 MHz. The links, constituting the GL High Latitude Meteor Scatter Test-Bed, are used to measure meteor scatter propagation and communication properties during quiet and disturbed ionospheric conditions. The propagation properties include: meteoric signal arrival rates, duty cycles, signal durations and fading rates. From these, communication properties such as throughput and waiting time for messages of

(Received for publication 30 July 1991)

1. Crysdale, J.H., (1960) Analysis of the performance of the Edmonton-Yellowknife JANET circuit, *IRE Trans. Com.*.
2. Maynard, L.A., (1961) Propagation of meteor burst signals during the polar disturbance of November 12-16 1960. *Can. J. Phys.* V39, p628.

given length can be derived for a range of postulated modulations and signaling protocols. Descriptions of the links, and the results obtained have been presented in a range of papers and reports.^{3,4,5,6,7,8,9,10} No SPE's occurred during the first years of operation of the test-bed. However, solar disturbances in March, April, August, September, and October 1989 provided both absorption events and large variations in solar noise. The data acquired during the March and August 1989 disturbances have been selected for presentation here, as they show a very illustrative combination of absorption and noise effects. An analysis incorporating all the disturbances of 1989 will be published later.

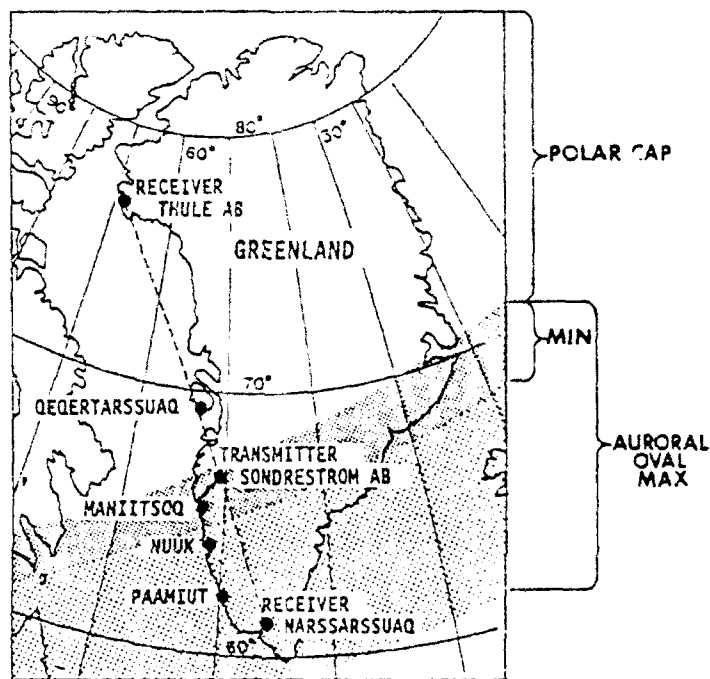


Figure 1. Geographical Locations of the GL High Latitude Meteor Scatter Test-Bed.

The absorption on a meteor scatter path during a PCA occurs in the lower D-region of the ionosphere in the height range of 45 to 85 km, well below the height of the meteor trails. The geometry of a communication path is shown in Figure 2. In general, the absorption A_{f1} for one pass through an absorbing layer at the fre-

3. Ostergaard, J.C., J.E. Rasmussen, M.S. Sowa, J.M. Quinn and P.A. Kossey, (1985) Characteristics of high latitude meteor scatter propagation over the 45 to 104 MHz band, *AGARD Conf. Proc.*, AGARD CP-382, paper 9.2.
4. Ostergaard, J.C., J.E. Rasmussen, M.S. Sowa, J.M. Quinn and P.A. Kossey, (1986) *The RADC High Latitude Meteor Scatter Test Bed*, RADC-TR-86-74, Rome Air Development Center, ADA180550
5. Weitzen, J.A. and S. Tolman, (1986) *A technique for automatic classification of meteor trails and other propagation mechanisms for the Air Force high latitude meteor burst test bed*, RADC-TR-86-117, Rome Air Development Center, AD173133.
6. Weitzen, J.A., (1987) A data base approach to analysis of meteor burst data, *Radio Science*, Vol. 22, No. 1, pp 133-140.
7. Weitzen, J.A., (1989) *USAF/GL Meteor scatter data analysis program. Users guide*, GL-TR-89-0154, ADA214988
8. Weitzen, J.A., M.J. Sowa, R.A. Scofidio, J. Quinn, (1987) Characterizing the multipath and doppler spreads of the high latitude meteor burst channel, *IEEE Trans. Com.* V.COM-35, no. 10.
9. Ostergaard J.C., (1987) Meteor Burst propagation and system design. Special course on interaction of propagation and digital transmission techniques. *AGARD R-744*.
10. Sowa, M.J., Quinn, J.M., Rasmussen, J.E., Kossey, P.A., Ostergaard, J.C., (1987) A statistical analysis of polar meteor scatter propagation in the 45 - 104 MHz Band. *AGARD Conf. Proc.*, AGARD-CP-419, paper 44.

quency f_1 and at an elevation angle of z can be approximated as:

$$A_{f1} = A_{f0} (f_0/f_1)^n \text{slant}(z) \text{ dB} \quad (1)$$

where f_0 is a reference frequency lower than f_1 , A_{f0} is the zenith absorption at f_0 , and n is an exponent describing the frequency dependence of the absorption. The exponent n has a value of approximately 2 for low values of absorption. $\text{slant}(z)$ is a factor describing the ratio between the path at zenith and the path elevated $90-z$ degrees. The factor would have been equal to the secant of the zenith angle if the earth were flat and the absorbing layer began at the surface (see Figure 3). However, due to the earth's curvature, the slant factor does not increase above 6 for an absorbing layer at 45 to 85 MHz. The absorption decreases with an increase in frequency, and increases with the length of the path through the absorbing region. The influence of the slant factor should be noted as the absorption values expressed in the above formula are in dB. Thus, a zenith absorption of 6 dB translates into a slant path absorption of 25 dB for a 10 degree elevation angle. A signal propagating between the stations of a meteor scatter link is attenuated twice; once propagating through the absorbing region of the ionosphere from the transmitter to the meteor trail and again from the meteor trail to the receiver. For a quiet site, the receiver noise power is dominated by galactic noise at low VHF frequencies, decreasing with frequency to the power -2.3. The noise is also absorbed by the ionosphere, but only through one passage of the absorbing region.

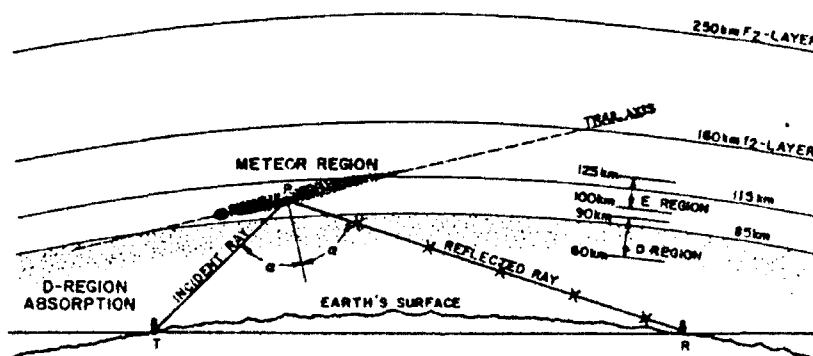


Figure 2. Cross Section of a Meteor Scatter Propagation Path.

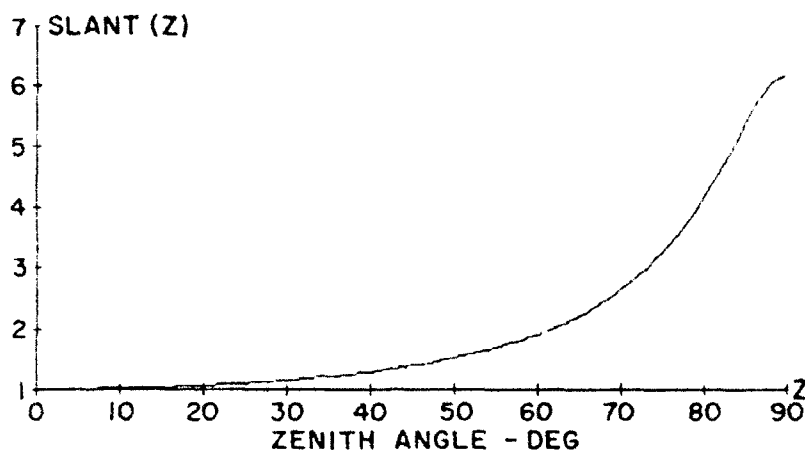


Figure 3. Ratio of Path Length at Zenith and at Zenith Angles in the Range 0 to 90 deg. Through the Ionosphere's D-region.

Thus, the higher frequencies are less affected by the absorption than the lower frequencies, but at the same time the higher frequencies offer less communication capacity during undisturbed ionospheric conditions. The frequency dependence of the capacity can be expected to decrease with frequency¹¹ to the power -2.7 . This exponent includes the effects of smaller scattering efficiency, shorter trail durations as frequency increases and a galactic noise limited receiving system. An optimum frequency of operation for a meteor scatter link must then exist for a given absorption level. This report presents and examines propagation data from the August 1989 PCA as a function of frequency in an effort to determine this relationship. The above simple relations are insufficient for an accurate quantification of the frequency dependence of absorption effects during PCA's and a more general review of ionospheric absorption is presented below prior to the discussion of the test-bed data.

2. IONOSPHERIC ABSORPTION AT VHF FREQUENCIES.

The properties of ionospheric absorption at VHF are presented in this section with a discussion of the dependence of absorption on collision frequencies, electron density profiles, wave frequency and the height of the absorbing region.

Following the presentation in (ref.12), the ionospheric absorption (A) in the D-region can be computed using the Appleton-Hartree formula as:

$$A = \text{Const} \int Nv / (v^2 + (w \pm w_L)^2) dS \quad (2)$$

where N is the electron density, v is the collision frequency, w is the wave angular frequency, w_L is the gyro angular frequency and dS is the incremental path length. This formula implies a constant collision frequency. The collision frequency is not constant however, so the formula cannot be used for accurate computation of the absorption. The equation is useful, however, to illustrate that the absorption is dependent on the electron density profile, the wave frequency and the collision frequency, and that the absorption follows a frequency-square relationship if the wave angular frequency is much larger than the collision frequency and the gyro frequency.

11. Eshlemann, V.R., (1957) On the wavelength dependence of the information capacity of meteor burst propagation. Proc. IRE.

12. K. Rawer ed., *Manual of ionospheric absorption measurements*. (1976) World Data Centre A Report UAG-57.

At VHF the wave frequency is much larger than the gyro frequency, but the collision frequency at altitudes between 45 and 60 km is of the same magnitude as the wave angular frequency. The frequency dependence of the absorption in this height range will therefore differ from the frequency-square relationship and will depend on the fraction of the total absorption that occurs in this height range. Sen and Wyller have formulated a generalized magneto-ionic theory that does not imply a constant collision frequency¹³. This theory provides more accuracy in the computation of the ionospheric absorption A at VHF frequencies:

$$A = \text{Const} \int N a/w C_{\frac{1}{2}}(a) ds \quad (3)$$

where N is the electron density, w the wave angular frequency, $a = w/v'$ and dS is the incremental path. $C_{\frac{1}{2}}(a)$ is one of a special class of integrals found in semiconductor theory. The values of these integrals can either be found in tables¹⁴ or computed. The value of the collision frequency v used in the expression has been discussed by Thrane and Piggott¹⁵.

The magnitude of the expected advantage of operating a meteor scatter communication systems at higher frequencies to overcome absorption is a function of the frequency dependence of the ionospheric absorption. A frequency dependence different from the simple frequency-square relationship depicted by the Appleton-Hartree formula for cases where the collision frequency is smaller than the wave angular frequency will reduce the advantage of the higher frequencies. A dependence of the absorption proportional to frequency or even independent of frequency, such as can be envisioned if the absorption exclusively occurs at a height range where the collision frequency is much higher than the wave angular frequency, would seriously limit or eliminate any advantage of operation at higher frequencies.

The ITSA raytracer¹⁶ modified to incorporate the Sen-Wyller formulation for the complex index of refraction in the ionosphere has been used to compute the zenith absorption at noon on 23 and 26 September, 1978. The computations, presented below, are aimed at examining the frequency dependence and height of occurrence of the ionospheric absorption during a PCA event. The computations are based on electron density profiles obtained from the GL oblique VLF ionosounder at Thule¹⁷ and collision frequency profiles presented by Thrane, and by Piggott and Friedrich^{13,18}. Figure 4 shows the electron density profiles and the collision frequency profile used for the computations. The increased ionization below 90 km, as compared to the quiet day profile, is clearly seen. The zenith absorption at 30 MHz was approximately 10 dB at noon on September 23 and approximately 3 dB at noon on September 26. The electron density increases two to four orders of magnitude below 55 km on the 23rd where the electron density exceeds $106/\text{m}^3$ at 48 km. The profile for the 26th shows little increase at 45 to 52 km but one to two orders of magnitude increase of the electron density in the range 55 to 65 km.

13. Sen, H.K., Wyller, A.A., (1960) On the generalization of the Appleton-Hartree Magnetoionic formulas. *J. Geophys. Res.* Vol 65, p 3931.

14. Dingle, R.B., D. Arndt, S.K. Roy, (1957) The integral $C_p(x)$ and $D_p(x)$ and their tabulation. *Appl. Sciences Res.* 6B p155.

15. Thrane, E.V., W.R. Piggott, (1966) The collision frequency in the E- and D-regions of the ionosphere. *J.A.T.P.* V30, p135.

16. Jones, R.M. (1975) *A versatile three dimensional raytracing computer program for radio waves in the ionosphere*. U.S. Dept. Commerce.

17. Fossey, P.A., J.P. Turtle, R.P. Pagliarulo, W.I. Klemetti, and J.E. Rasmussen, (1983) VLF reflection properties of the normal and disturbed polar ionosphere in northern Greenland. *Radio Sci.* Vol. 18, No. 6, p. 907-916.

18. Friedrich, M., K.M. Torkar, (1983) Collision frequencies in the high latitude D region. *J.A.T.P.* V45, p267.

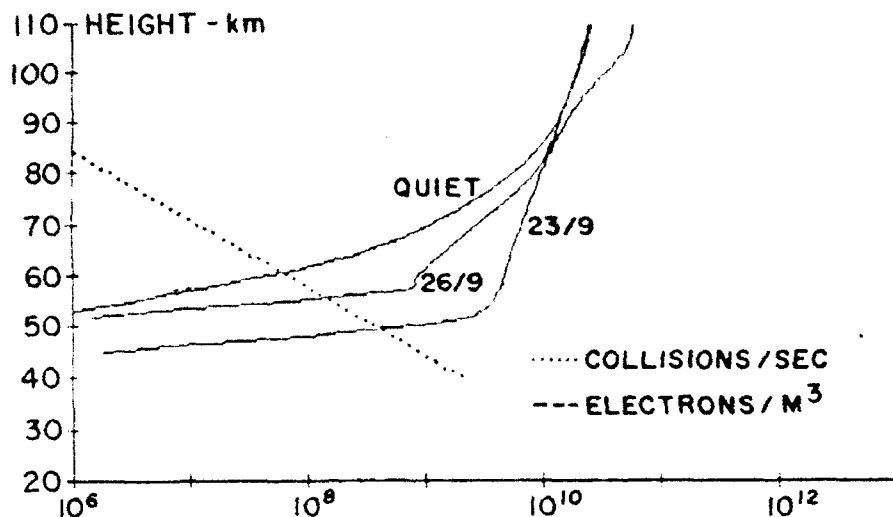


Figure 4. Electron Density Profiles at Noon on 23 and 26 Sept. 1978 at Thule.

The collision frequency profile is presumed independent of the increased ionization. The temperature of the D-region is not increased more than a few degrees Kelvin during even large particle events (E.V. Thrane personal communication.) and such changes will introduce negligible changes in the collision frequency. Figures 5 and 6 show the computed cumulative and specific absorption at noon on September 23, 1978 as a function of height and frequency. The cumulative absorption increases as expected with height and more than 80% of the absorption occurs below 80 km. Significant absorption takes place between 48 and 55 km where the collision frequency is high relative to the wave angular frequency. As the meteor trails occur between approximately 85 and 110 km, the absorption takes place below the meteor region. The specific absorption is largest at 60 km for a wave frequency of 30 MHz and it decreases both in magnitude and altitude with an increase in frequency. This is expected, as the maximum absorption should occur at altitudes where the wave angular frequency is comparable to, or smaller than, the collision frequency. Figures 7 and 8 show the computed cumulative and specific absorption at noon on September 26, 1978 as a function of height and frequency. The absorption is less than at noon on the 23rd and occurred below 90 km. The maximum specific absorption at 30 MHz occurred at 65 km and little change is seen between 55 and 75 km. The height of the maximum specific absorption still decreases with frequency but very little absorption takes place below 55 km. Thus, the absorption mainly occurred between 60 and 90 km on the 26th of September when the total zenith absorption was approximately 3 dB, and between 55 and 85 km on the 23rd when the total zenith absorption was approximately 10 dB. This means that the absorption is not totally dominated by the increased ionization below 60 km. The increased ionization above 60 km contributes a large part of the total absorption, even at an absorption level of 10 dB.

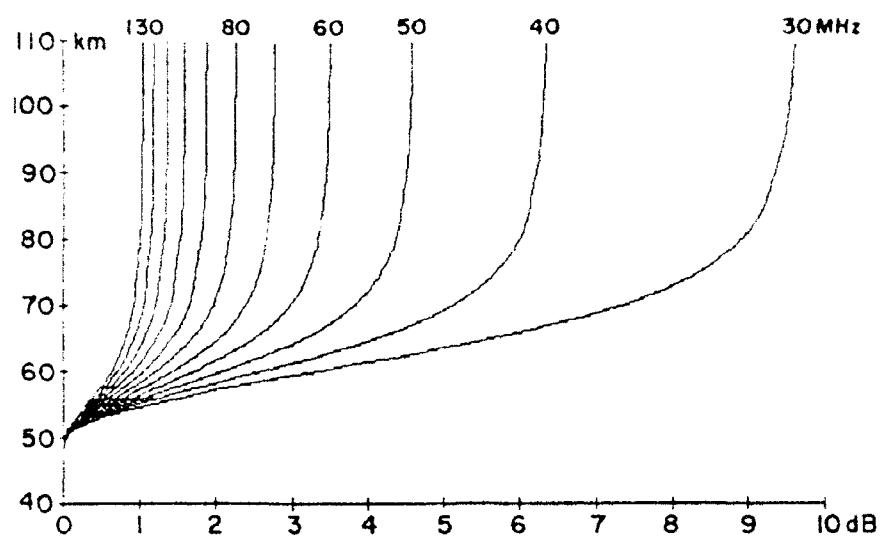


Figure 5. Computed Cumulative Zenith Absorption at Noon 23 Sep. 1978.

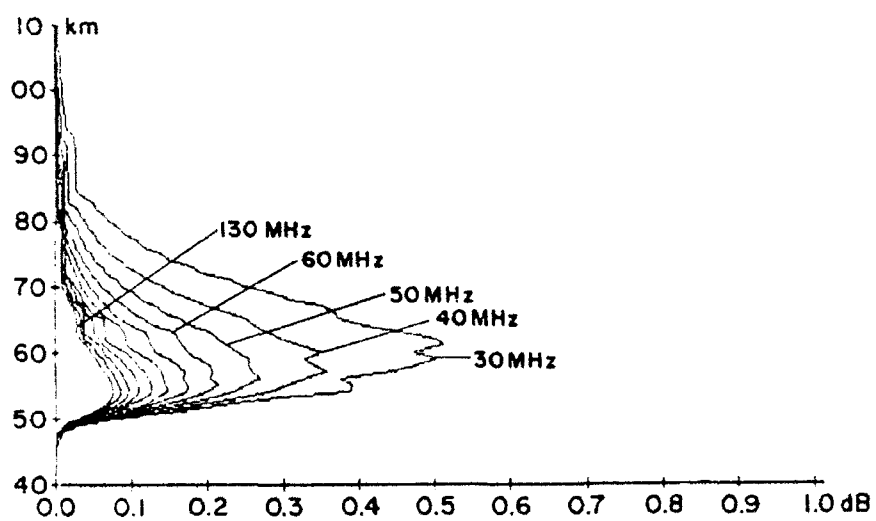


Figure 6. Computed Specific Zenith Absorption at Noon 23 Sep. 1978.

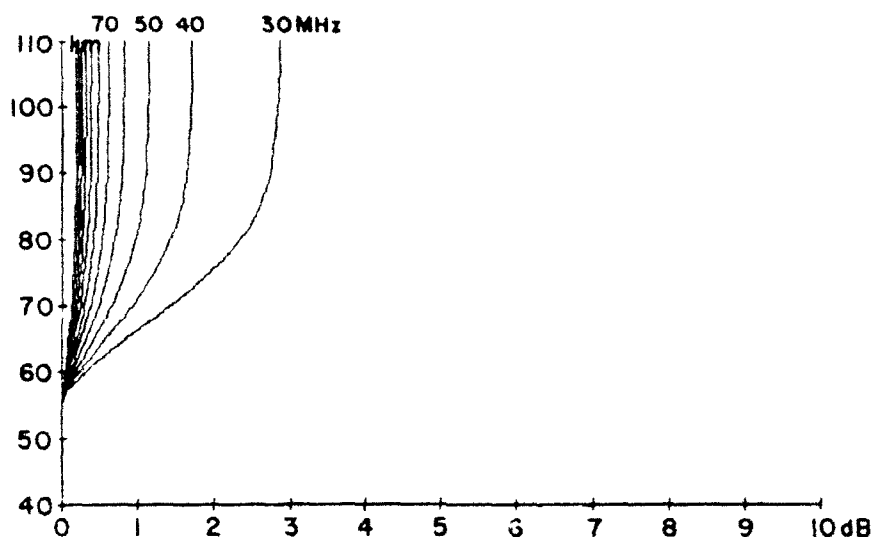


Figure 7. Computed Cumulative Zenith Absorption at Noon 26 Sep. 1978.

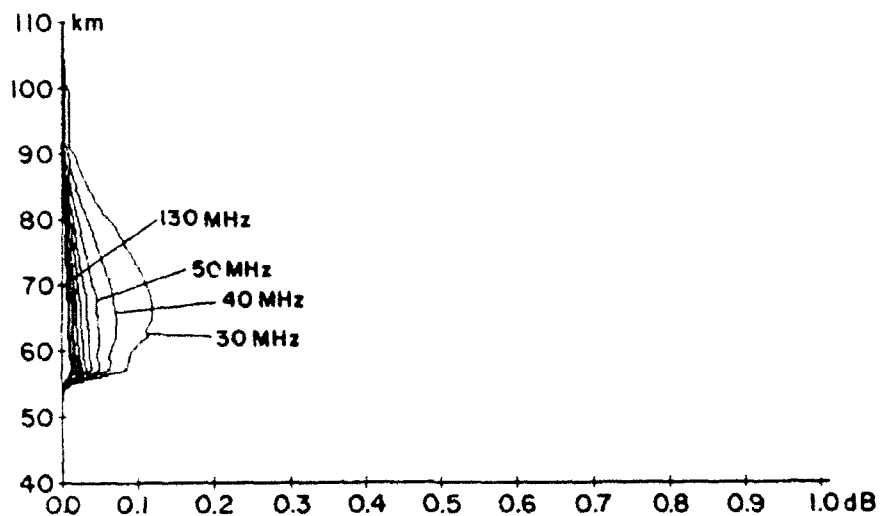


Figure 8. Computed Specific Zenith Absorption at Noon 26 Sep. 1978.

The frequency dependences of the cumulative absorption at noon on 23 and 26 September 1978 are presented as functions of frequency and height in Figures 9 and 10. The absorption decreases with increasing frequency at all heights as expected. Also, the rate of decrease is least at the lower heights, and is not linear with frequency when presented in double logarithmic coordinates. The rate of decrease of absorption with frequency gets larger with height, and also more linear. If the slopes of the curves were linear then an exponent describing the frequency dependence of the absorption could be determined for each height. Analysis of such exponents have been presented by Lerfald and Little¹⁹ in the frequency range 5 to 50 MHz. The slope is not linear however, and adoption of fixed exponents to describe the frequency dependence of absorption must be accompanied by a description of the frequency range and method of fitting used to determine the slope. The expo-

ment for the same absorption event can vary considerably for different frequency ranges. Although not strictly valid, the concept of an exponential fit to the frequency dependence of absorption can be useful for analysis of absorption data. The following exponents have been derived as a linear fit to the absorption in the frequency range 30 - 100 MHz:

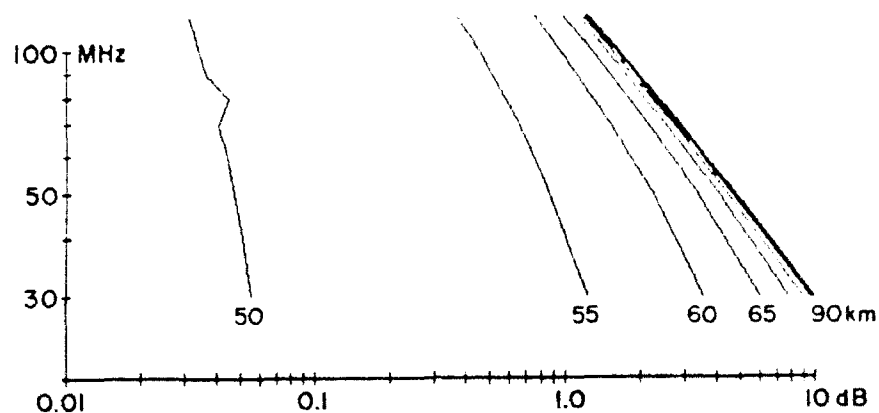


Figure 9. Computed Frequency Dependence of the Cumulative Absorption at Noon 23 Sep. 1978.

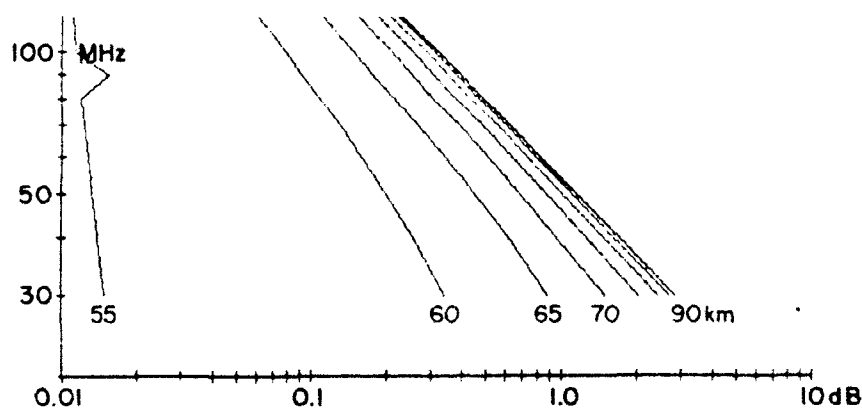


Figure 10. Computed Frequency Dependence of the Cumulative Absorption at Noon 26 Sep. 1978.

19. Lerfeld, G.M., C.G. Little, (1964) D-region electron density profiles during Auroras. *J. Geophys. Res.* V69 no 13.

At noon on the 23rd the computed absorption at 50 km is almost independent of frequency, as the collision frequency is comparable to or greater than the wave angular frequency. However, the cumulative absorption at this height is only a small fraction of the total absorption. At 60 km, the absorption is almost inversely proportional to frequency, and at 90 km the absorption varies as frequency to the power -1.5. At noon on the 26th, the absorption is almost frequency independent at 55 km, and close to a frequency-square dependency at 90 km. The variations of the exponents with height for the two days are presented in Figures 11 and 12. The differential exponent increases from 0 to 2 in the height range from 50 to 70 km. The cumulative exponent reaches a value of 1.5 and 1.8 respectively for the two cases. The overall exponent is lower on the 23rd because more of the total absorption occurred below 60 km on this date compared to the 26th. In both cases, absorption occurring above 60 km constitutes a large part of the total absorption and the overall exponent cannot be totally dominated by the low values found between 45 and 60 km.

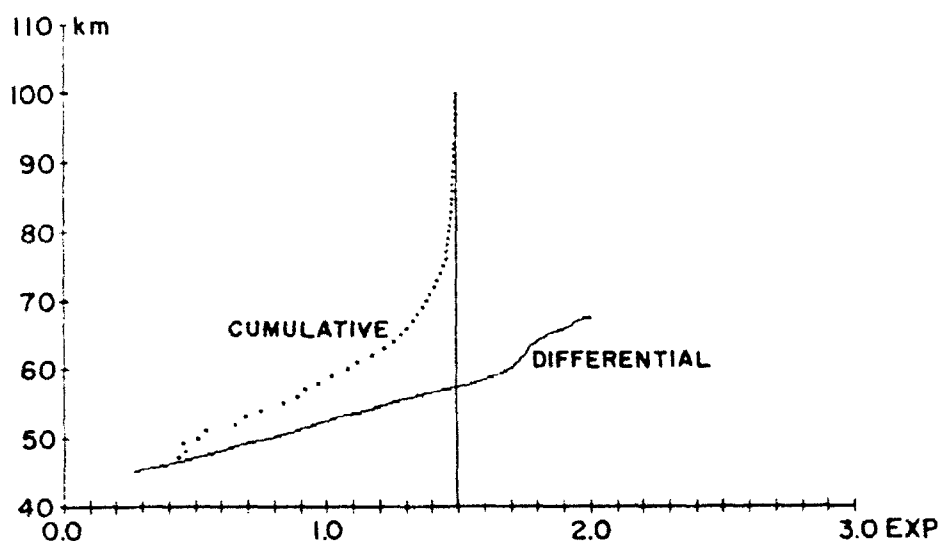


Figure 11. Computed Exponent of Frequency Dependence of Absorption vs. Height at Noon 23 Sep. 1978.

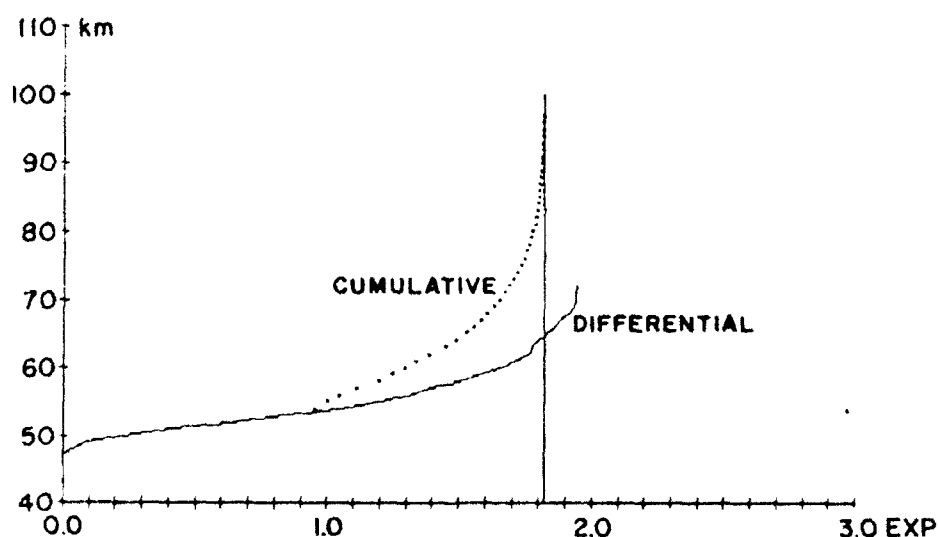


Figure 12. Computed Exponent of Frequency Dependence of Absorption vs. Height at Noon 26 Sep. 1978.

The two examples shown here do not cover all possible electron density profiles that can be expected during solar proton events, but they are believed to phenomenologically represent a wide range of absorption conditions. These can be summarized as follows: The ionospheric absorption during a PCA event occurs in the height range from 45 to 80 km. The larger absorption levels contain substantial contributions from the lower part of this range, whereas the lower absorption levels are dominated by absorption in the range 60 - 75 km. Although an exponential fit to the frequency dependence of the absorption is strictly not valid, such exponents derived for the frequency band 30 to 100 MHz range from -2 at very low levels of absorption to -1.5 or less when the absorption exceeds 10 dB at 30 MHz. However, the exponent of -1.5 observed during the 10 dB absorption of September 23rd, indicates that the absorption level is unlikely to become frequency independent even during very high naturally occurring absorption levels.

3. MEASUREMENT OF IONOSPHERIC ABSORPTION AT VHF

Ionospheric absorption is usually measured with a riometer operating at 30 MHz. The principles of riometers and their use is described in a range of excellent references²⁰ and only a few aspects of the use of riometers, especially important for measurement of large absorption values such as encountered during PCA's, will be mentioned here. A riometer is basically a power meter connected to an antenna pointed at zenith, and the absorption A_{riometer} is measured as:

$$A_{\text{riometer}} = 10 \log(P_{\text{abs}}/P_{\text{quiet}}) \text{ dB} \quad (4)$$

where P_{quiet} is the power measured at the antenna feed point during quiet ionospheric conditions, and P_{abs} is the power measured during an absorption event. Power can be measured either in Watts (P) or in degrees Kelvin (T) where $P = kTBw$, k is Boltzmann's constant ($1.38 \times 10^{-23} \text{ W/Hzdeg}$) and Bw is the bandwidth of the power meter. Temperature as a power measure is conveniently independent of bandwidth and will be used in the following, implying this relation between power and temperature exists. The diurnal variation of the noise during quiet ionospheric conditions is termed the quiet day curve, and is used as a reference for the absorption measurements. At 30 MHz the noise of an antenna pointed at zenith is of galactic origin at a quiet receiving site, so the decrease in the measured noise is due to absorption in the ionosphere. Friedrich²¹ has determined the ionospheric absorption at 30 MHz during quiet ionospheric condition to be approximately 0.01 dB, which is insignificant for the absorption measurement.

The riometer installation, including antenna, is not a completely linear instrument with respect to the magnitude of the galactic noise power at zenith. The riometer itself has a dynamic range determined by the dynamic range of the variable noise source in the riometer. This has a lower limit set by the physical temperature of the termination resistor in the noise source, approximately 290 - 300 K. The upper limit is set by the excess noise ratio of the noise source, but this is usually much higher than the highest level of galactic noise. The output voltage from the riometer is usually the DC voltage across the termination resistor of the noise source, or other measure of the DC current flowing through it. It is usually assumed that the output voltage of the riometer is proportional to the noise temperature at the antenna feed point less 290 K. This assumption is valid for riometers using temperature limited vacuum tube diodes as noise sources, but may not be valid for riometers using variable solid state diodes. Experience with the GL riometers at Thule shows that it is advisable to check

20. Cormier, R.J., (1970) *Riometry as an aid to ionospheric forecasting*, AFCRL TR 70-0689, AD721182

21. Friedrich, M., K.M. Torkar, (1983) High latitude plasma densities and their relation to riometer absorption. *J A T P*, V45, p217.

the calibration of solid state riometers with a primary noise standard before use.

A moderate gain antenna such as a five element Yagi or an array of two element Yagis is often used with riometers. The computed radiation pattern for the riometers at Thule is shown in Figure 13. The main beam of the antenna is pointed towards zenith, but the -3 dB beam width is approximately 50 degree. Thus, galactic noise arriving at zenith angles in the range from 0 degrees to beyond 25 degrees will contribute to the noise temperature of the antenna. Due to the extra length of the path through the ionosphere, noise arriving at angles different from zenith will suffer greater absorption than noise arriving at zenith. The absorption measured by the riometer is then larger than the absorption at zenith. Also, the noise temperature of the ionosphere itself contributes to the antenna temperature. The electron temperature of the ionosphere in the height range where the absorption takes place²² is 200 - 270 K, and the antenna temperature, T_{ant} , is determined as:

$$T_{ant} = T_{gal}A + (1-A)T_{ionosphere} \quad (5)$$

where A is the value of the absorption and $T_{ionosphere}$ is the temperature of the ionosphere. For small values of A the ionospheric temperature introduces insignificant errors in the measurement of absorption as the galactic noise temperature (T_{gal}) is in the range of 7000 K to 10,000 K. The ionospheric contribution gains significance as the absorption increases. Figure 14 shows the ratio between the measured absorption and the zenith absorption in dB for the Thule riometer with the ionospheric temperature as a parameter. The ratio, which is dependent on the radiation pattern of the antenna used, is approximately 1.3 at low values of absorption, consistent with the value found in the literature¹². It decreases with an increase in absorption. The slope of the curves change at approximately 5 dB zenith absorption from being dominated by the antenna pattern beam width to being dominated by the influence of the ionospheric temperature. At approximately 13 - 15 dB zenith absorption the measured absorption is equal to the zenith absorption and at higher values the zenith absorption is larger than the measured absorption. If the ionosphere is envisioned as an opaque screen, and the galactic noise as a uniform source of light, then the light pattern seen by the riometer antenna during an absorption event will grow gradually darker at the circumference than at the center of the field of view of the antenna until it obtains a uniform darkness corresponding to the radiation caused by the ionospheric temperature.

22. COSPAR International Reference Atmosphere (1972), Akademik-Verlag, Berlin.

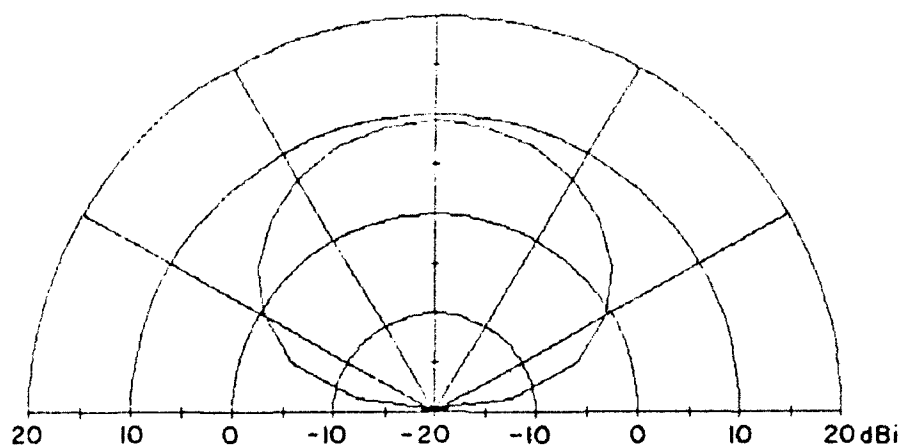


Figure 13. Computed Radiation Pattern for the Riometer at Thule AB.

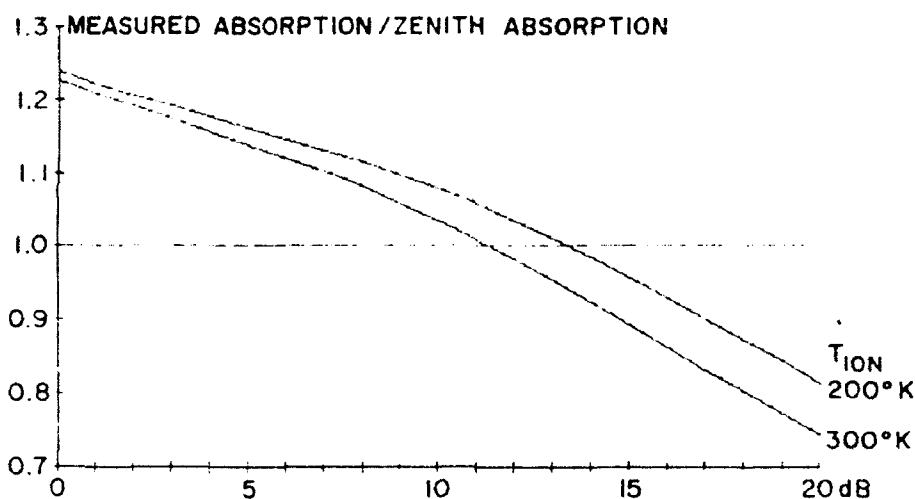


Figure 14. Ratio of Measured Absorption and Zenith Absorption in dB at Thule AB.

The conclusion of the above discussion is that the term 'riometer absorption' as used in the literature may be very different from 'zenith absorption' during large PCA events, and suitable corrections must be included before riometer data can be used for accurate determination of absorption levels during such events. A detailed analysis of these corrections is presented in Ref. 23. The absorption measurements presented in this report have been corrected for the influence of antenna patterns, feeder cable losses and noise source non-linearities. An ionospheric temperature of 200 K has been assumed and the absorption values represent the zenith absorption to the accuracy of the corrections.

23. Ostergaard, J.C., Derivation of zenith absorption from riometer measurements with special emphasis on the GL riometers at Thule AB., in publication.

4. THE INFLUENCE OF PCA'S ON SYSTEM NOISE

The noise in a meteor scatter receiving system is composed of galactic noise, receiver front end noise and man made noise and interference. For a properly designed system, man made noise and interference can be completely suppressed leaving only the receiver noise and the galactic noise. The receiver noise temperature for a properly constructed receiver should not exceed 500 K throughout the frequency range 30 - 150 MHz. The average galactic noise temperature is a function of frequency ranging from 10,000 K at 30 MHz to 250 K at 150 MHz. Also, the galactic noise contribution to a receiving system, that is, the receiving antenna temperature, is the sky noise temperature integrated over the antenna aperture. This is a function of the antenna gain and the noise temperature vs azimuth and elevation and the properties of the terrain below the antenna.

The computed elevation pattern at boresight for the horizontally polarized, five element, 45 MHz Yagi antenna used with the test-bed receiver at Thule AB is shown in Figure 15. The antenna is mounted 1.5 wavelengths above the ground to obtain optimum illumination of the common scattering volume between Sondrestrom and Thule²⁴. The radiation properties of the antenna itself were computed from the dimensions and spacings of the antenna elements using the method of moments. A computer program originating from the Technical University of Denmark, specifically tailored for analysis of Yagi antennas, was used²⁵, but other programs such as NEC²⁵ could have been used as well. Next the radiation pattern of the antenna mounted above the partially reflecting ground in Thule was computed using the complex Fresnel reflection coefficients for the ground. The resulting antenna gain shows an increase of 5 dB at an elevation angle of 8 degrees relative to the free space gain of the antenna. This added gain, caused by the ground reflection, is highly advantageous for the operation of the link, as it increases the received signal power from meteor trails near the hot spots close to the midpoint of the link. The antenna gain at elevation angles exceeding approximately 25 degrees is of no consequence for the reception of meteor scatter signals from Sondrestrom, as these all arrive at lower elevation angles. However, the antenna noise temperature, being the galactic noise temperature integrated over the antenna aperture, contains contributions originating from all elevation angles. During undisturbed ionospheric conditions this temperature is dominated by the galactic noise arriving at low elevation angles within the main beam of the antenna where the gain is largest. The galactic noise arriving at low elevation angles will be absorbed more than the noise arriving at high elevation angles during a PCA event, as the low elevation angle paths must traverse a much longer path through the absorbing region of the ionosphere. Consequently, the galactic noise seen by the high elevation sidelobes will contribute a larger and larger part of the antenna noise temperature as the absorption level increases. This means that the antenna temperature cannot be expected to decrease much more than the zenith absorption at a given frequency.

24. Hald, J., J.E. Hansen, (1982) *Dipole Arrays With Loading Networks*. Electromagnetics Institute Rep. R257, R258, Technical University of Denmark.

25. NEEDS, The Numerical Electromagnetic Engineering Design System. Version 1.0 February 1988. Dist. by the Applied Computational Electromagnetics Society.

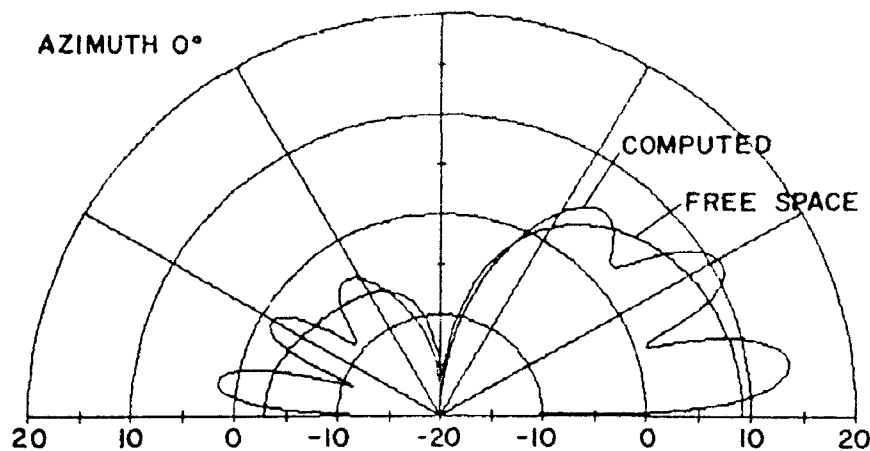


Figure 15. Computed Radiation Pattern for the 45 MHz Meteor Scatter Antenna at Thule AB.

This mechanism favors operation at the higher frequencies during absorption events as both signal and noise are absorbed less than at the lower frequencies. A large signal absorption at the lower frequencies would not be detrimental to the operation of a meteor scatter link if the noise was absorbed by the same amount as the signal, but the channel capacity at low frequencies will not only suffer from the much larger signal absorption as the signal traverses the absorbing region twice and the noise only once, but the noise originating from the high angle sidelobes of the receiving antenna will further limit the capacity. Also, the ionospheric temperature eventually limits the antenna temperature to values greater than 200 - 300 K at all frequencies. The obtainable lower limit is finally influenced by the receiver noise, but this can easily be reduced to approximately 100 K, a value which will not impair the operation of the receiving system. Thus, higher gain antennas with low sidelobes may be particularly advantageous for long meteor scatter links if resistance to absorption is important, not only due to the gain but also due to the reduced sidelobe noise contribution.

Although a receiver noise temperature of 100 K is technically feasible, it may not be possible to exploit it at the lower frequencies, because absorption levels so high that the antenna temperature decreases to 200 - 400 K most certainly will be accompanied by large signal path losses, so large that the meteor signals will have all but disappeared before the antenna temperature has decreased to this point. A noise figure of 3 dB (290 K) is easily obtained with standard transistors. This noise figure will be sufficiently low for systems operating at 30 - 50 MHz and with effective radiated transmitter powers of 10 - 20 kW. At higher frequencies such as 80 - 100 MHz, a lower noise figure may be of use to make sure the receiver noise does not at any instant degrade the sensitivity of the receiving system.

5. THE AUGUST 1989 PCA

A major solar proton event occurred in the middle of August 1989. The associated polar cap absorption began in the afternoon of the 12th and reached a maximum 30 MHz zenith absorption of 13 dB around noon on the 13th as shown in Figure 16. The absorption then decreased throughout the 13th and 14th to reach a low of 2 dB at midnight on the 14th and then increased again to reach another maximum of 7 dB at noon on the 16th. The absorption reached a third maximum of 2.5 dB at midnight on the 19th and then decreased until noon on the 20th when the event ended.

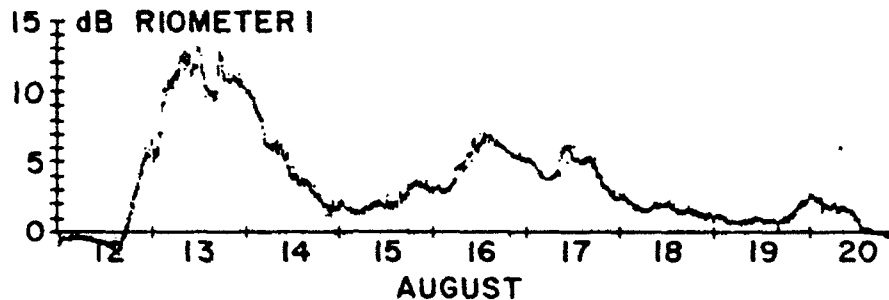


Figure 16. Zenith Absorption Measured at Thule AB, 10 to 22 Aug 1989.

The receiver noise absorption at the six frequencies of the Thule meteor scatter receiver during the period 10 to 23 August is presented in Figure 17. Absorption (that is, a decrease in receiver noise) is represented with positive numbers, and an increase in noise by negative numbers. The days leading up to the event show noise increases ranging from 4 to 8 dB at all frequencies. The largest increases are found at 104 MHz. Similar noise increases are found at Narssarssuaq and must be associated with the early stages of the event. The 35 MHz record shows large noise increases throughout the period of the PCA, as well as noise absorptions. These noise increases appear at Thule in the early spring and disappear in the late fall. Their first occurrence in the spring of 1989 coincided with the sharp increase in the sunspot number. Their origin is unknown, but they are believed to be interference propagated into Thule by F2-layer reflections south of the area affected by the absorption. Such signals are known from North East Greenland where HF paths at 18 MHz or higher are regularly open to Europe during PCA's.

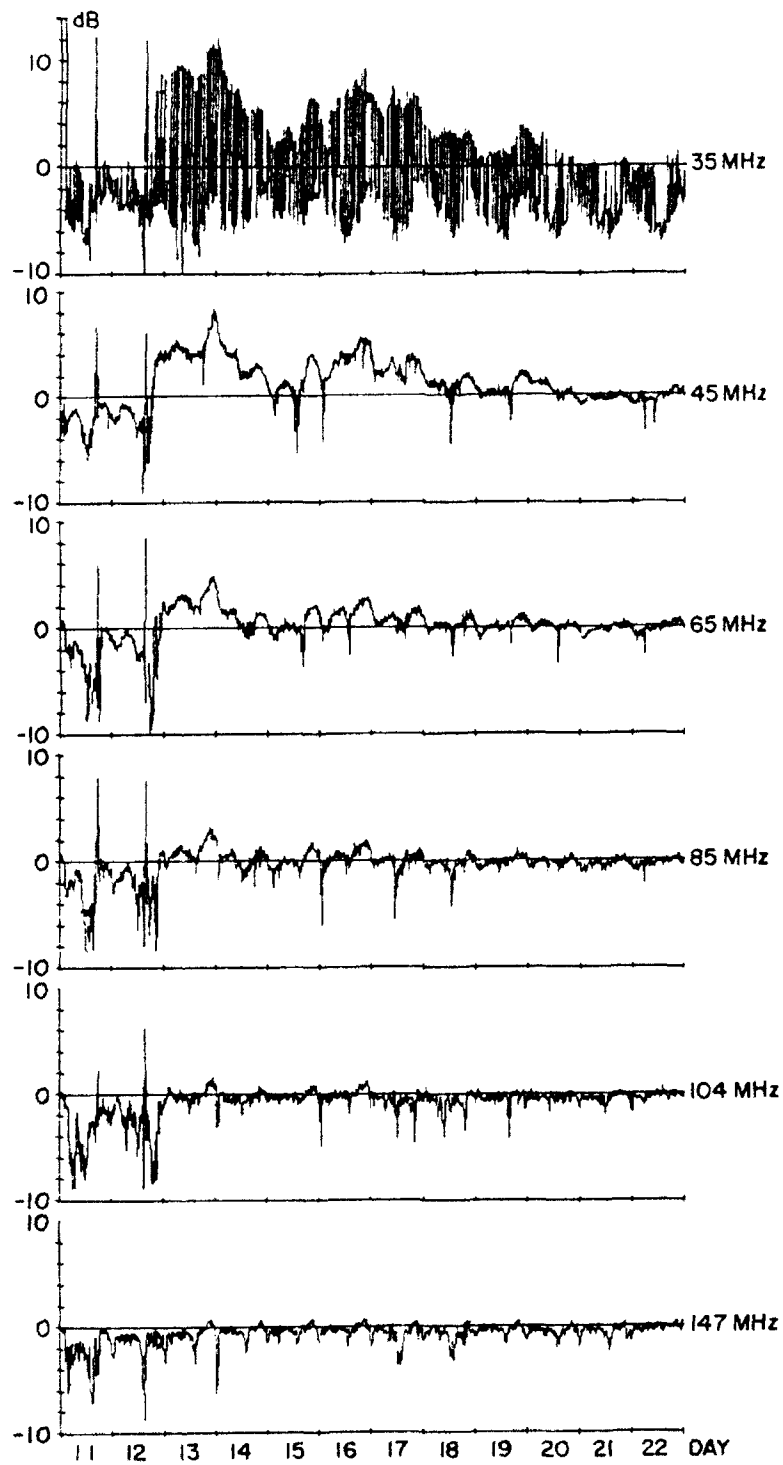


Figure 17. Measured Noise Absorption at 35, 45, 65, 104 and 147 MHz at Thule AB Aug. 1989.

Solar X-ray emissions are known to create strong radio noise bursts at the beginning of a PCA and such emissions are most probably the cause of the enhanced receiver noise occurring at all frequencies between noon and midnight on the 12th. The noise absorption increases to a sharp maximum of 12 dB at 35 MHz and 8 dB, 4 dB and 2 dB at 45, 65, and 85 MHz respectively on the afternoon on the 13th. Little noise absorption is seen at 104 and 147 MHz. The maximum 30 MHz zenith absorption was 12 - 13 dB but the noise levels at the receiver frequencies did not decrease much more than the expected zenith absorption at the respective frequencies. This confirms the result of the discussion presented above that the receiver noise cannot be expected to decrease much more than the zenith absorption value at any frequency even at very high absorption levels.

The meteoric arrival rate and the duty cycle for August 1989 for signals exceeding - 116 dBm at Thule are shown in Figures 18 and 19. The arrival rate at 35 MHz was very intermittent due to dominating sporadic E-layer propagation at this frequency. The arrival rates for the other frequencies ranged from an average of approximately 6 meteors/min at 45 MHz to an average of 1, 0.3, 0.2, and 0.08 meteors/min at 65, 85, 104, and 147 MHz respectively. Large diurnal and day-to-day variations were observed during the undisturbed periods. The effect of the absorption was clearly seen. The link was interrupted at frequencies below 104 MHz during most of the 13th and decreased arrival rates were seen throughout the duration of the PCA event. The decrease was frequency dependent with the largest decreases occurring at 35, 45, and 65 MHz. Much smaller decreases were seen at the higher frequencies (85, 104, and 147 MHz). 104 MHz was not interrupted, but the arrival rate decreased slightly during the 13th and 14th. The arrival rate at 147 MHz is generally very small, and it often happens that no trails are detected within a 20 min measurement period. The arrival rate is therefore undefined regularly even during quiet ionospheric conditions and it was not possible to differentiate between the interruptions due to a small arrival rate and those due to absorption during the PCA. During the period from 11 to 13 August a slight increase in the arrival rate was seen twice a day on all frequencies except 35 MHz. This was due to the Perseid meteor shower that peaks in this period.

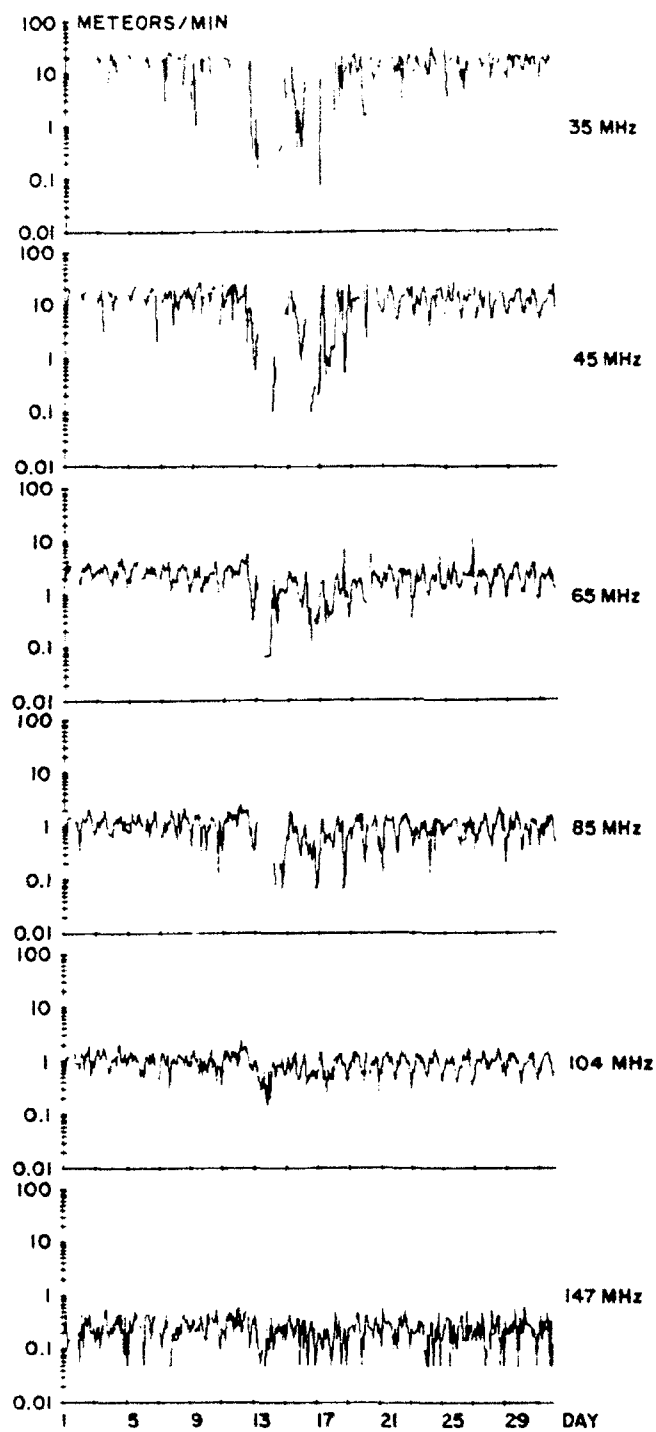


Figure 18. Meteor Trail Arrival Rate Exceeding -116 dBm Signal Level at Thule AB Aug. 1989.

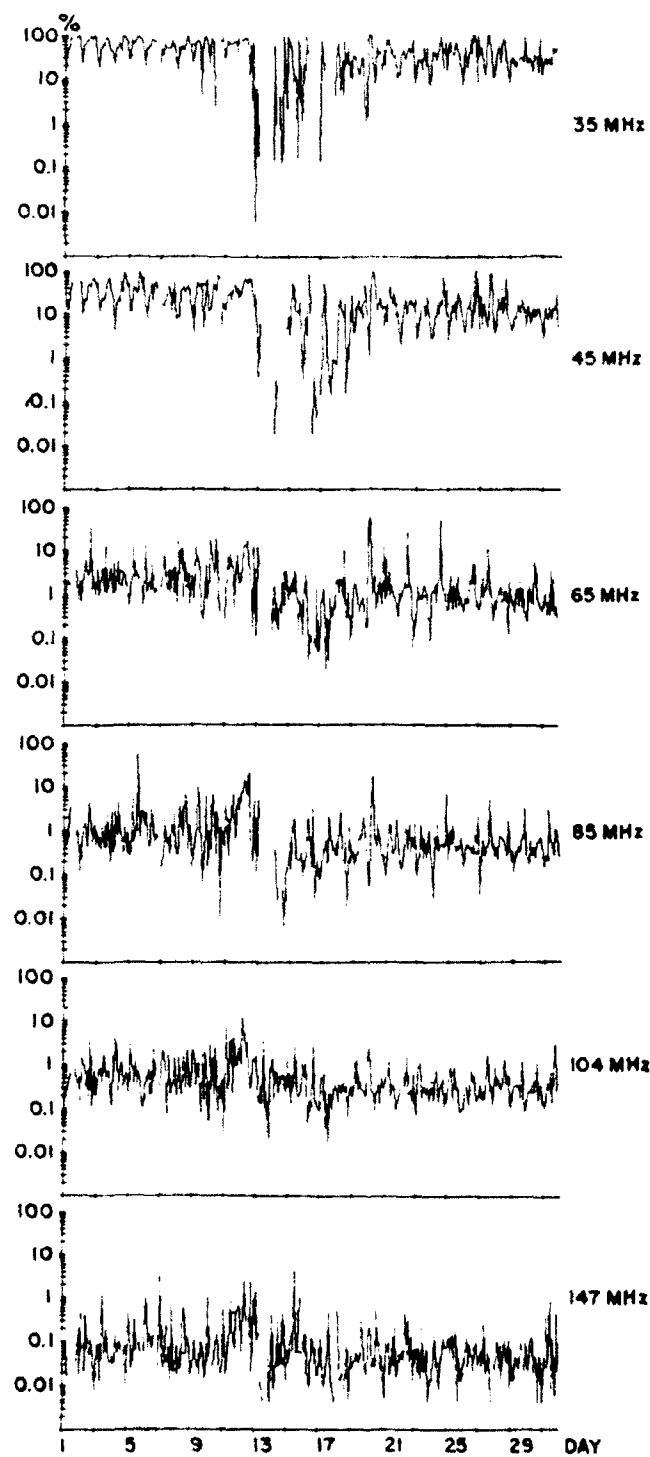


Figure 19. Duty Cycle Exceeding -116 dBm at 35, 45, 65, 104, and 147 MHz at Thule Aug. 1989.

The duty cycle, which is a measure of the average communication capacity, shows much larger diurnal and day to day variations than the arrival rates, often exceeding an order of magnitude during the quiet periods. This must be kept in mind when assessing the influences of absorption on the communication capacity. In calculating the duty cycle statistics shown in Figure 19, the sporadic E-layer contribution is included and is the reason for the 100 percent values at 35 MHz. The contribution of the Perseid shower was more clearly observed in the duty cycle statistics than in the arrival rates, especially at 85 and 104 MHz. The duty cycle was also very frequency dependent during the PCA event. The largest decreases are seen at 35, 45, and 65 MHz, whereas smaller decreases are seen at 85 and 104 MHz. The changes observed at 147 MHz during the PCA were predominantly increases rather than decreases. They were most likely due to the Perseid shower meteors and it appears that the absorption had very little effect at 147 MHz.

The duty cycle obtained for optimum selection of the operating frequency for a SNR of 17 dB on the Sondrestrom-Thule link during the PCA event is shown in Figure 20. The frequencies are 45, 65, 85, 104, and 147 MHz. 35 MHz has been eliminated, as this frequency was dominated by sporadic E-layer propagation, and the contribution of the meteor trails was very difficult to assess. The chosen frequencies and the zenith absorption at 30 MHz are also shown. The best frequency of operation was 45 MHz whenever the zenith absorption was less than 3.5 dB and 104 MHz was chosen when the zenith absorption exceeded approximately 10 dB. 65 and 85 MHz were selected to cover the intermediate range. The highest frequency, 147 MHz, was rarely selected except during the very short times when the zenith absorption reached its maximum on the 23rd and when strong noise bursts were present at the lower frequencies. The absorption was very frequency dependent and the link was never totally interrupted, but the duty cycle dropped almost two orders of magnitude from 15 to 0.15 percent during the most intense parts of the absorption when frequencies lower than 104 MHz were interrupted. This change seems very large, but it mostly reflects the difference between the average duty cycle at 45 and 104 MHz during quiet ionospheric conditions. It should be noted that interruptions at the lower frequencies occurred at higher levels of absorption than the levels of absorption where the frequency changes took place, and 104 MHz was not interrupted at all. If only 45 and 104 MHz were available, the link could still be sustained, although with a somewhat decreased capacity for zenith absorptions in the range of 5 to 8 dB.

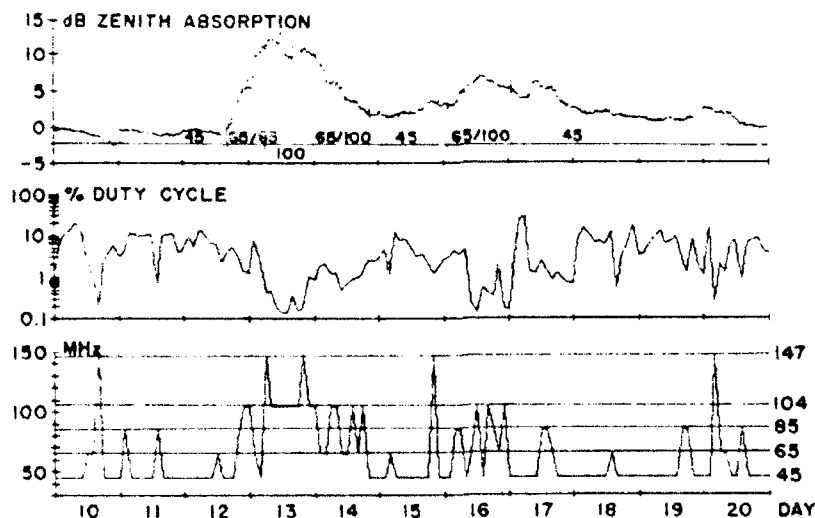


Figure 20. Duty Cycle and Frequency of Operation for Optimum Selection of Frequency Compared to Zenith Absorption Aug. 10 to 20 1989.

6. THE MARCH 1989 PCA

Two solar disturbances occurred in March 1989. The zenith absorption at 30 MHz for the period 9 to 22 March is shown in Figure 21. A polar cap absorption was observed beginning March 9 and ending March 13. The zenith absorption at 30 MHz reached values between 1 and 3 dB except for a few hours at noon on the 13th when the absorption reached 6 dB. A very large solar flare occurred on the 17th and the associated zenith absorption at 30 MHz reached 7 dB in the early afternoon of the 18th and disappeared around midnight on the 20th.

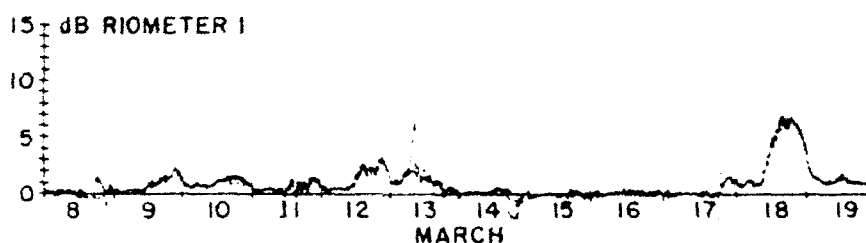


Figure 21. Zenith Absorption Measured at Thule AB March 1989.

The noise absorption for the six frequencies of the Sondrestrom-Thule link are shown in Figure 22. Positive numbers denote absorption and negative numbers an increase in the receiver noise relative to the undisturbed noise level. The solar flare on the 18th produced a marked noise absorption of 6 dB at 35 MHz, 4 dB at 45 MHz and 2 dB at 65 MHz. Very little absorption is observed at the higher frequencies. The PCA that occurred between March 9 and 13 should not have caused appreciable noise absorption due to the low level of zenith absorption. This indeed is true. Only the absorption peak at noon on the 13th resulted in discernable absorption at 35, 45, 65, and 85 MHz. Very large increases of the receiver noise were observed, however, on all frequencies around noon in the period 10 through 16 March. The increases were smallest at 35 MHz, being less than 10 dB, but exceeded 15 dB at all other frequencies. The occurrence and disappearance of the noise was coincident with the local sunrise and sunset at Thule. The receiving antennas at Thule were pointed to the south, and it was very apparent that the noise was present only when the sun was in view of the antennas. A 104 MHz antenna pointing north did not receive the noise except for a short period around sunrise and sunset when the sun was within view of the antenna sidelobes.

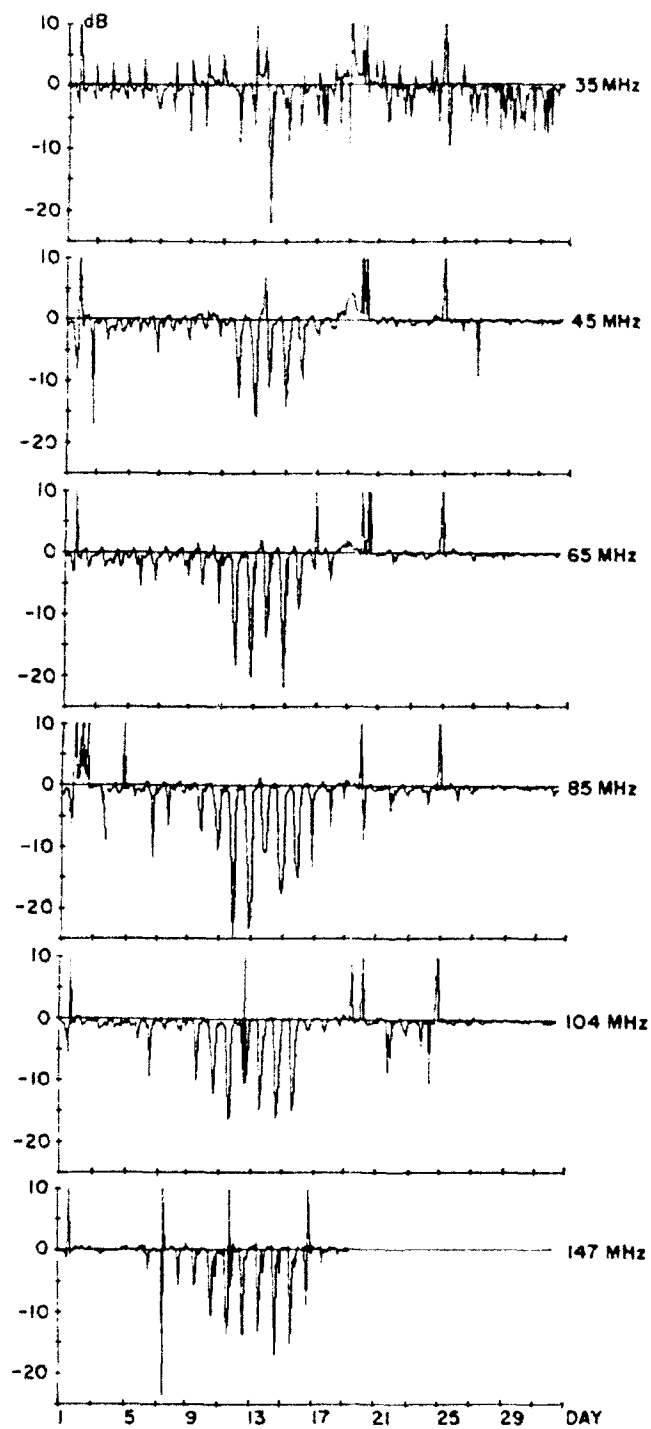


Figure 22. Measured Noise Absorption at 35, 45, 65, 85, 104, and 147 MHz, Thule AB March 1989.

The meteoric arrival rates and duty cycles for March 1989 are presented in Figures 23 and 24. Both the absorption and the increase in receiver noise caused the arrival rates and duty cycles to decrease. The 7 dB zenith absorption associated with the solar flare caused interruption at 35 and 45 MHz, whereas the higher frequencies experienced smaller decreases as the frequency increased. At 65 MHz the arrival rate dropped by a factor of 15 from 1.5 meteors/min to 0.1 meteors/min and the duty cycle dropped from 0.8 to 0.03 percent. At 85 MHz the arrival rate and duty cycle dropped from 0.8 to 0.1 meteors/min and 0.3 to 0.03 percent respectively. Even less changes were seen at 104 MHz where the arrival rate dropped from 0.8 to 0.3 meteors/min and the duty cycle from 0.2 to 0.08 percent. The influence of the absorption was clearly frequency dependent. The influence of the solar noise emissions on the other hand, decreased the arrival rates and duty cycles approximately two orders of magnitude at all frequencies. The effect was largest at 65, 85, and 104 MHz, consistent with the large solar noise power increases at these frequencies. The 30 MHz zenith absorption at the time of the solar noise bursts did not exceed 2 - 3 dB and therefore the effects of the disturbance were dominated by the solar noise emissions. This would not have been the case if the links were oriented from Thule to Sondrestrom as the receiving antennas would have been pointed north and the receiver noise would not have increased significantly due to the solar noise emissions. The disturbance would still have caused absorption on the path, but the channel capacity would only have been reduced by the absorption. The channel capacity of the two links if operated in a duplex mode would have been strongly influenced by the large reduction suffered by the south-to-north link as link management would be very difficult or impossible with one of the links having a channel capacity approximately two orders of magnitude lower than the other.

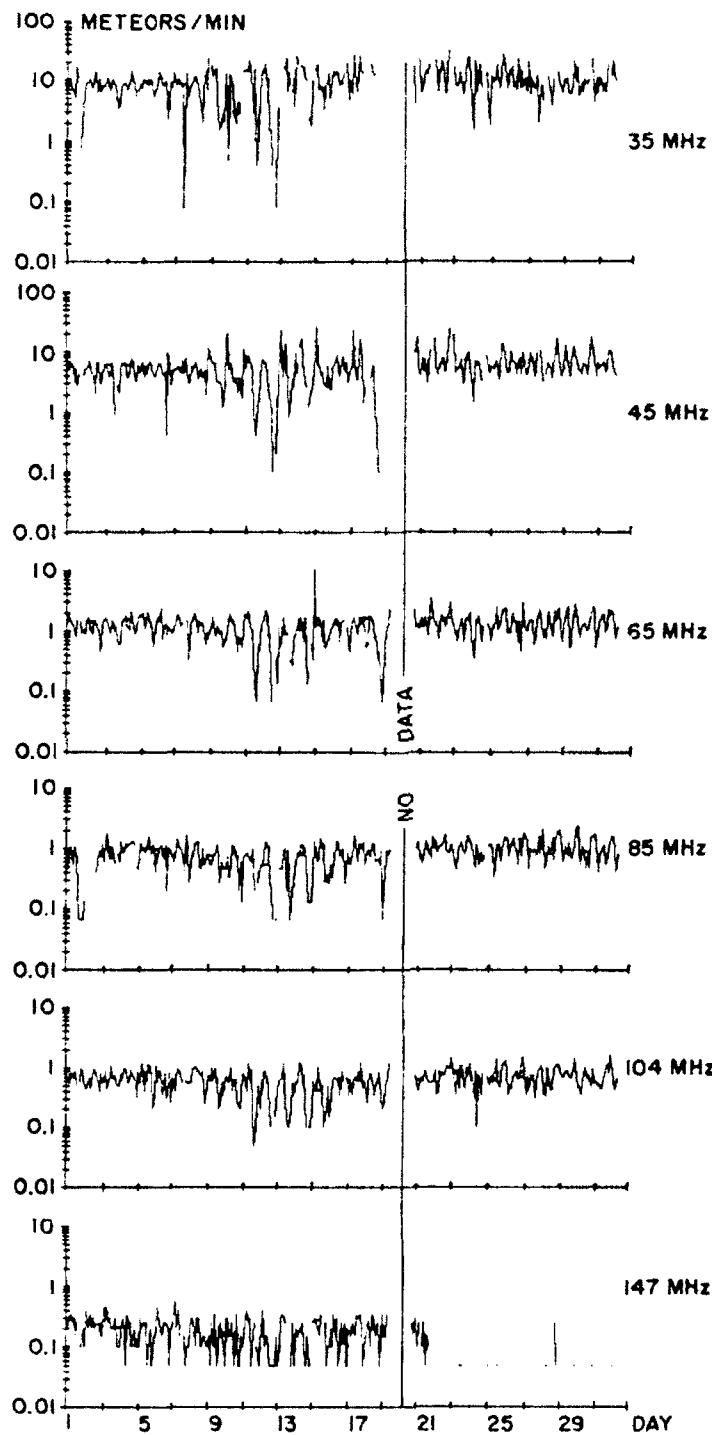


Figure 23. Meteor Trail Arrival Rate Exceeding -116 dBm Signal Level at 35, 45, 65, 85, 104, and 147 MHz
Thule AB August 1989.

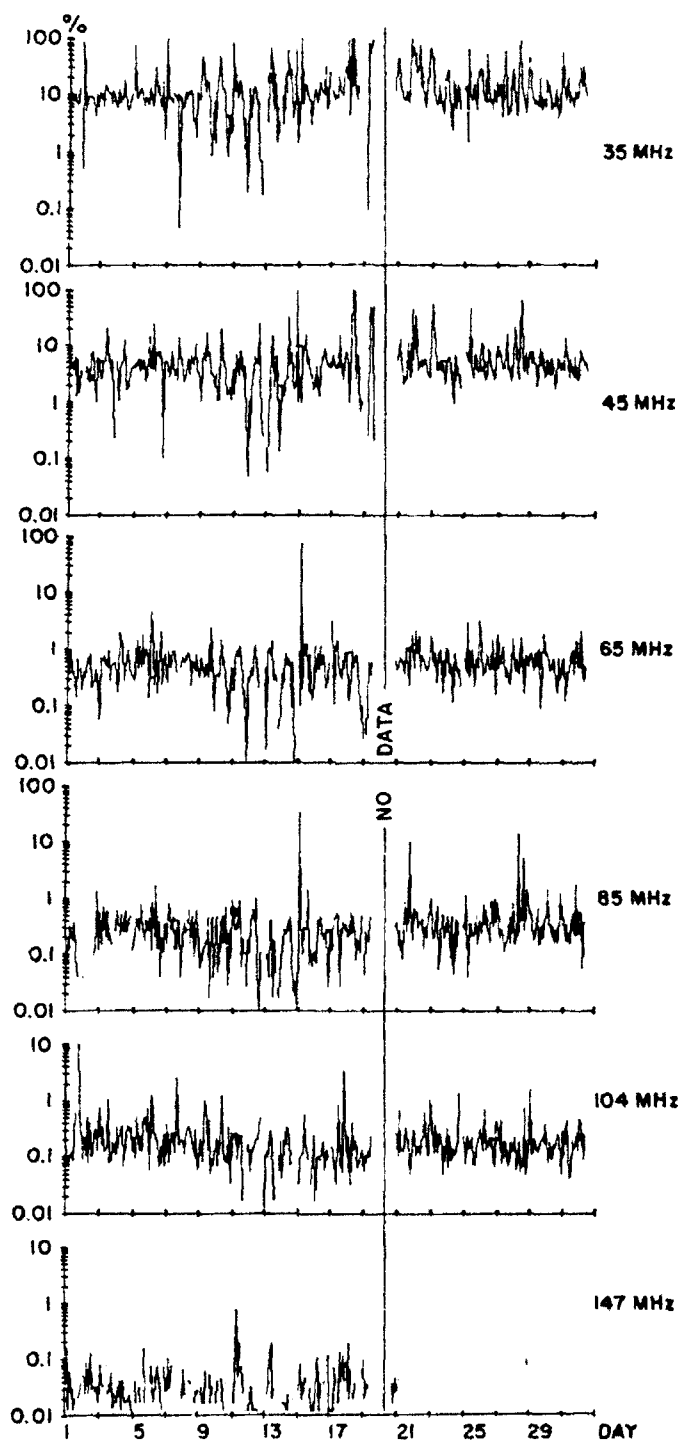


Figure 24. Duty Cycle Exceeding -116 dBm Signal Level at 35, 45, 65, 85, 104, and 147 MHz
Thule AB August 1989.

The existence of strong solar noise emissions in the VHF band has been known to geophysicists for many years, but it has received little attention in conjunction with meteor scatter propagation evaluations. The solar temperature is very high compared with the ambient galactic noise temperature even during undisturbed ionospheric conditions but the spatial extent of the sun is too small to influence the antenna temperature for the five to ten element Yagi antennas often used with a meteor scatter links. The fact that the noise emitted by the sun being a point source during the March event exceeded the undisturbed level by 10-25 dB indicates that the noise temperature of the sun must have increased by several orders of magnitude. The noise emissions were apparently not accompanied by a large flux of high energy protons as the ionospheric absorption did not exceed 3 dB during most of the event. The August PCA on the other hand had high levels of absorption but few solar noise emissions. Also, communication systems using FM modulations such as frequency shift keying have limiting IF amplifiers in the receivers. The demodulated noise level from such receivers does not change with a change of the antenna temperature, so link degradations are easily ascribed to signal loss rather than to noise increase unless separate noise measurements are performed.

The influence of the November 1960 SPE on the performance of the JANET meteor scatter system operating in Northern Canada² indicate that both the 45 and the 104 MHz links were interrupted extensively by the event. Riometer absorption in excess of 18 dB was reported for the early parts of the event, and this level of absorption would certainly have strongly influenced both frequencies. However, strong solar noise emissions in the VHF spectrum were also reported for this event. The SPE effects on both of the JANET links has stimulated speculation that absorption on meteor scatter systems would be frequency independent during PCA's, eliminating the advantage of working at higher frequencies. It may be, however, that the interruption of the 104 MHz link was not caused by absorption as much as by the increased solar noise.

SUMMARY

Data acquired with the 1200 km GL High Latitude Meteor Scatter Test-Bed between Sondrestrom AB and Thule AB in Greenland during solar disturbances in March and August of 1989 have been analyzed and presented. The solar disturbance of August 1989 resulted in a Polar Cap Absorption event reaching 12 dB zenith absorption at 30 MHz. The test-bed, operated at 35, 45, 65, 85, 104, and 147 MHz, was significantly influenced by the absorption. All frequencies lower than 104 MHz were interrupted for periods ranging from a few hours to one day during the part of the event when the zenith absorption exceeded 10 dB. No interruptions occurred at 104 MHz although a slight decrease of duty cycle was noted. The absorption was highly frequency dependent. Operation at frequencies in the range 65 to 104 MHz outperformed 35 and 45 MHz during the most severe absorption. The solar disturbances in March 1989 produced a weak PCA with a maximum zenith absorption of 3 dB. Little effect was seen from the absorption, but very strong solar noise bursts decreased the signal-to-noise ratio on all frequencies and caused interruptions. It is speculated that solar noise bursts present during previous Solar Proton Events could have been the basis for expectations that the absorption at VHF frequencies during these events was frequency independent. That is not supported by the results presented in this report.

References

1. Crysdale J.H., (1960), Analysis of the performance of the Edmonton-Yellowknife JANET circuit, *IRE Trans. Com.*
2. Maynard, L.A., (1961) Propagation of meteor burst signals during the polar disturbance of November 12-16 1960. *Can. J. Phys.* V39, p628.
3. Ostergaard, J.C., J.E. Rasmussen, M.S. Sowa, J.M. Quinn and P.A. Kossey, (1985) Characteristics of high latitude meteor scatter propagation over the 45 to 104 MHz band, *AGARD Conf. Proc.*, AGARD-CP-382, paper 9.2.
4. Ostergaard, J.C., J.E. Rasmussen, M.S. Sowa, J.M. Quinn and P.A. Kossey, (1986) *The RADC High Latitude Meteor Scatter Test-Bed*, RADC-TR-86-74, Rome Air Development Center. ADA180550.
5. Weitzen, J.A. and S. Tolman, (1986) *A technique for automatic classification of meteor trails and other propagation mechanisms for the Air Force high latitude meteor burst test bed*, RADC-TR-86-117, Rome Air Development Center, AD173133.
6. Weitzen, J.A., (1987) A data base approach to analysis of meteor burst data, *Radio Science*. Vol. 22, No. 1, pp 133-140.
7. Weitzen, J.A., (1989) *USAF/GL Meteor scatter data analysis program. Users guide*. GL-TR-89-0154. ADA214988
8. Weitzen, J.A., M.J. Sowa, R.A. Scofidio, J. Quinn, (1987) Characterizing the multipath and doppler spreads of the high latitude meteor burst channel, *IEEE Trans. Com.* V.COM-35, no. 10.
9. Ostergaard J.C., (1987) Meteor Burst propagation and system design. Special course on interaction of propagation and digital transmission techniques. AGARD R-744.
10. Sowa, M.J., Quinn, J.M., Rasmussen, J.E., Kossey, P.A., Ostergaard, J.C., (1987) A statistical analysis of polar meteor scatter propagation in the 45 - 104 MHz Band. *AGARD Conf. Proc.*, AGARD-CP-419, paper 44.
11. Eshleemann, V.R., (1957) On the wavelength dependence of the information capacity of meteor burst propagation. *Proc. IRE*.
12. K. Rawer ed., (1976) *Manual of ionospheric absorption measurements*. World Data Centre A Report UAG-57.
13. Wyller, A.A., Sen, H.K., (1960) On the generalization of the Appleton-Hartree Magnetoionic formulas. *J. Geophys. Res.* Vol 65, p 3931.
14. Dingle, R.B., D. Arndt, S.K. Roy, (1957) The integral $C_p(x)$ and $D_p(x)$ and their tabulation. *Appl. Sciences Res.* 6B p155.
15. Thrane, E.V., W R. Piggott, (1966) The collision frequency in the E- and D-regions of the ionosphere. *J.A.T.P.* V30, p135.
16. Jones, R.M. (1975) *A versatile three dimensional raytracing computer program for radio waves in the ionosphere*. U.S. Dept. Commerce.
17. Kossey, P.A., J.P. Turtle, R.P. Pagliarulo, W.I. Klemetti, and J.E. Rasmussen, (1983) VLF reflection properties of the normal and disturbed polar ionosphere in northern Greenland, *Radio Sci.* Vol. 18, No. 6, p. 907-916.
18. Friedrich, M., K.M. Torkar, (1983) Collision frequencies in the high latitude D-region. *J.A.T.P.* V45, p267.
19. Lerbald, G.M., C.G. Little, (1964) D-region electron density profiles during Auroras. *J. Geophys. Res.* V69 no.13.
20. Cormier, R.J., (1970) *Riometry as an Aid to Ionospheric Forecasting*, AFCRL TR-70-0689. AD721182.
21. Friedrich, M., K.M. Torkar, (1983) High latitude plasma densities and their relation to riometer absorption. *J.A.T.P.* V45, p217.
22. *Cospar International Reference Atmosphere* (1972), Akademie-Verlag, Berlin.

21. Friedrich, M., K.M. Torkar, (1983) High latitude plasma densities and their relation to riometer absorption. *J.A.T.P.* V45, p217.
22. *Cospar International Reference Atmosphere* (1972), Akademie-Verlag, Berlin.
23. Ostergaard, J.C., Derivation of zenith absorption from riometer measurements with special emphasis on the GL riometers at Thule AB., in publication.
24. Hald, J., J.E. Hansen, (1982) *Dipole arrays with loading networks*. Electromagnetics Institute Rep. R257, R258, Technical University of Denmark.
25. *NEEDS, The Numerical Electromagnetic Engineering Design System. Version 1.0* February 1988. Dist. by the Applied Computational Electromagnetics Society.